Proceedings of the 2006 IEEE/RSJ
International Conference on Intelligent Robots and Systems
October 9 - 15, 2006, Beijing, China

Static Walk of a Humanoid Robot Based on the Singularity-Consistent Method

K. Takahashi, M. Noda and D. N. Nenchev
Department of Mechanical Systems Engineering
Musashi Institute of Technology
Tamazutsumi 1-28-1, Setagaya-ku, Tokyo
158-8557 Japan

Y. Tsumaki and A. Sekiguchi
Department of Intel. Machines and System Eng.
Hirosaki University
3 Bunkyo-cho, Hirosaki, Aomori
036-8561 Japan

***Abstract*— This paper addresses the problem of naturally looking and energy efficient walk of biped humanoids. We presuppose that such walk requires motion control capability around kinematic singularities, such that the knee can be fully extended. This problem is tackled by adopting the Singularity-Consistent method devoloped for manipulator motion control at and around kinematic singularities. We implemented the method with a HOAP-2 humanoid robot, demonstrating stable static walk as a first step in this direction.**

I. Introduction

Walking motion generators for biped humanoids make extensive use of the Zero-Moment Point (ZMP) concept [1]. ZMP is used for both motion planning and feedback control [2], [3]. Note, however, that the inverse kinematics for the legs has then to be calculated which may lead to problems related to kinematic singularities. An example of such singularity is the extended-leg configuration. It is well known that excessive joint velocities will be generated around a kinematic singularity. To avoid this, most humanoid robots walk without fully extending their legs. This leads to an unnatural appearance, and most important, to inefficiency due to energy loss in the knee joint. We have addressed this problem in earlier papers [4], [5]. Various aspects of the same problem are treated in [6]–[8].

Our approach to generate a naturally looking, energy-efficient walk is first to ensure inverse kinematics based control capability around and at kinematic singularities, and more specifically, around the extended-leg configuration. A possible approach, based on the Singularity-Consistent (SC) method, developed in our previous studies for manipulator control [9], has been introduced in [10], within a static walk framework. It must be noted that the SC method overcomes the singularity approach/depart problem by reducing the end-effector speed along the path. This may lead to a difficulty when implementing the method for humanoids, as shown in the above paper. Here, we tackle the problem by introducing a hybrid control scheme, taking advantage of the SC method to solve the inverse kinematics for the upper/lower leg kinematic subchain, and controlling the rest of the leg joints in joint space.

II. Background

The Singularity-Consistent method developed earlier to tackle manipulator motion control around and at kinematic singularities is briefly described below.

The velocity $\boldsymbol{v}$ of a characteristic point on the end-effector, and the angular velocity $\boldsymbol{\omega}$ of the end-effector can be obtained from the well known relation:

$$\begin{bmatrix} \boldsymbol{v} \\ \boldsymbol{\omega} \end{bmatrix} = \boldsymbol{J}(\boldsymbol{q})\dot{\boldsymbol{q}}, \tag{1}$$

where $\boldsymbol{J}(\boldsymbol{q})$ is the manipulator Jacobian and $\boldsymbol{q}$ is the joint variable vector, of dimension n, for an n-joint manipulator. The pair $(\boldsymbol{v}, \boldsymbol{\omega}) \equiv \boldsymbol{\nu} \in \Re^6$ represents the coordinates of the *end-effector twist*.

When the end-effector moves along a smooth parameterized path $\boldsymbol{x}(q_*)$, q_* denoting the path parameter, then the twist at a given point q_* can be represented as

$$\boldsymbol{\nu}(q_*, \dot{q}_*) = \boldsymbol{t}_*(q_*)\dot{q}_* \tag{2}$$

where $\boldsymbol{t}_*(q_*)$ is the normalized end-effector twist, obtained when the speed of the parameter is one: $\dot{q}_* = 1$. Equation (1) is then rewritten as:

$$\boldsymbol{t}_*(q_*)\dot{q}_* = \boldsymbol{J}(\boldsymbol{q})\dot{\boldsymbol{q}} \tag{3}$$

or

$$\boldsymbol{J}(\boldsymbol{q})\dot{\boldsymbol{q}} - \boldsymbol{t}(q_*)\dot{q}_* = \boldsymbol{0}. \tag{4}$$

This form of the equation gives us a hint: it would be convenient to augment the configuration space with the path parameter q_*. Thus, we obtain the *augmented configuration space* $\mathcal{C}^*$, a subspace of $\Re^{n+1}$, with elements $\bar{\boldsymbol{q}} \equiv (\boldsymbol{q}, q_*)$. Equation (4) can be rewritten in compact form, as:

$$\boldsymbol{H}(\bar{\boldsymbol{q}})\dot{\bar{\boldsymbol{q}}} = \boldsymbol{0} \tag{5}$$

where

$$\boldsymbol{H}(\bar{\boldsymbol{q}}) \equiv \begin{bmatrix} \boldsymbol{J}(\boldsymbol{q}) & -\boldsymbol{t}_*(q_*) \end{bmatrix}$$

is called *the column-augmented Jacobian*.

It should be apparent that Eq. (5) is underdetermined, and hence, the number of solutions is infinite. But this is also a homogeneous equation, then all the solutions must be in the kernel of matrix $\boldsymbol{H}$. Let us assume now that the manipulator is *nonredundant*: $m = n$. For a full-rank column-augmented Jacobian, the kernel will contain a single nonzero element then. The set of solutions of Eq. (5) is:

$$\dot{\bar{\boldsymbol{q}}} = b\bar{\boldsymbol{n}}(\bar{\boldsymbol{q}}) \tag{6}$$

1-4244-0259-X/06/$20.00 ©2006 IEEE

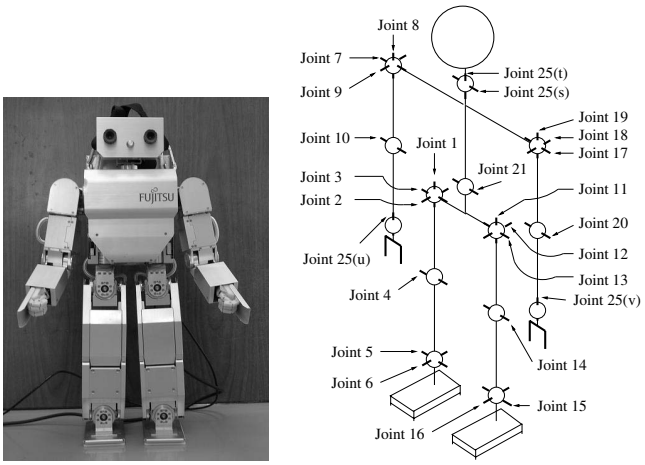

Fig. 1. HOAP-2 photo and kinematic structure

where b is an arbitrary scalar, and $\bar{\boldsymbol{n}}(\bar{\boldsymbol{q}}) \in \ker \boldsymbol{H}(\bar{\boldsymbol{q}}) \subset \Re^{n+1}$ can be written as:

$$\bar{\boldsymbol{n}}(\bar{\boldsymbol{q}}) \equiv \left[\begin{array}{cc} \boldsymbol{n}^T(\bar{\boldsymbol{q}}) & \det \boldsymbol{J}(\boldsymbol{q}) \end{array} \right]^T \tag{7}$$

where $\boldsymbol{n}(\bar{\boldsymbol{q}}) \equiv [\mathrm{adj}\boldsymbol{J}(\boldsymbol{q})]\, \boldsymbol{t}_*(q_*)$, adj$(\circ)$ denoting the adjoint matrix [11].

Equation (6) can be split into two parts to obtain joint differential motion

$$\dot{\boldsymbol{q}} = b\, \boldsymbol{n}(\bar{\boldsymbol{q}}) \tag{8}$$

and path parameter differential

$$\dot{q}_* = b \det \boldsymbol{J}(\boldsymbol{q}). \tag{9}$$

In conventional approaches, path parameter q_* is considered an independent variable. Then, one calculates the scalar b from Eq. (9), and substitutes it back into Eq. (8) to obtain the joint velocity. Note however, that this may not work in the vicinity of kinematic singularities where the determinant of the Jacobian is close to zero.

Under the Singularity-Consistent method, the roles of q_* and b are exchanged such that b becomes the new independent variable, while q_* is regarded as the dependent one. Then, from Eq. (9) it becomes apparent that the end-effector twist magnitude $\dot{q}_*$ will be zero at a kinematic singularity, since the determinant is zero. Note that when the Jacobian is singular and in addition, linear system (1) is inconsistent, a nontrivial solution can be obtained only when the end-effector is (instantly) at rest, i.e. the twist is set to zero. This condition must be satisfied in order to comply with the existing physical motion constraint at the singularity [9].

Eq. (8) has been called the *singularity-consistent inverse kinematic solution*.

III. Singularity-Consistent Inverse Kinematics of a Humanoid

We will apply the Singularity-Consistent method to a humanoid robot called HOAP-2 (see Fig. 1). It is a small size robot (50 cm tall), developed by Fujitsu Automation corporation as an experimental platform for research [12].

A. Kinematic structure of HOAP-2 legs

The two legs have identical kinematic structure. Each leg has six DOF's distrubuted as follows: three DOF's in the waist joint, one DOF in the knee joint and two DOF's in the ankle joint.

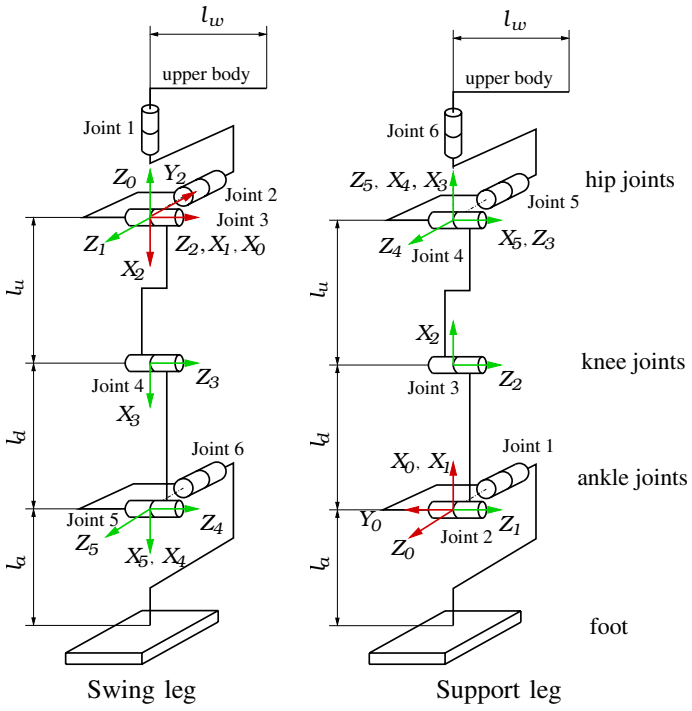

Fig. 2. Coordinate frames of the legs.

Two different singularity-consistent inverse kinematics solutions will be derived because each of the legs will be treated either as the swing leg or as the support leg. For this purpose, coordinate frame assignment according to Denavit and Hartenberg's method is done separately for the swing leg and the support leg (see Fig. 2). Also, joints will be renumbered for better understanding.

B. Singularity-consistent method applied to the swing leg

To obtain a computationally efficient solution, we consider frame $O_2X_2Y_2Z_2$ as the base frame of the swing leg. The Jacobian is then obtained by differentiating the following equation w.r.t. time:

$$\boldsymbol{T}_5^0 = (\boldsymbol{A}_0^1)^{-1}\ (\boldsymbol{A}_1^2)^{-1}\ \boldsymbol{A}_3^2\ \boldsymbol{A}_4^3\ \boldsymbol{A}_5^4 \tag{10}$$

where $\boldsymbol{T}$ and $\boldsymbol{A}$ are homogeneous transforms relating the coordinate frames who's numbers appear as subscripts and superscripts.

Henceforth, we apply the Singularity-Consistent method following the order described in Section II. The final result is the null space vector for the swing leg, denoted as $\boldsymbol{n}^{sw}$,

with components:

$$\begin{aligned} n_1^{sw} &= -t_z\, S_4 S_{345} \\ n_2^{sw} &= t_z\, C_2 C_{345}\, S_4 \\ n_3^{sw} &= 2C_\alpha\{C_2\, C_{\alpha 5}(t_x\, C_{34} + t_y\, S_{34}) + t_z\, S_2 S_{345}\} \\ n_4^{sw} &= -4C_2\, C_\alpha^2\, C_{\alpha 5}(t_x\, C_{3\alpha} + t_y\, S_{3\alpha}) \\ n_5^{sw} &= 2C_2\, C_\alpha\, C_{\alpha 5}(t_x\, C_3 + t_y\, S_3) \\ n_6^{sw} &= -t_z\, C_2 S_4 \end{aligned} \tag{11}$$

$S_{(\circ)}$ and $C_{(\circ)}$ stand for $\sin(\circ)$ and $\cos(\circ)$, respectively, and the subscripts denote joint numbers according to Fig. 2, multiple subscripts denoting sums of the respective joint angles, with α standing for $q_4/2$. t_x, t_y and t_z are the first three coordinates of twist $\boldsymbol{t}$ denoting the direction (unit vector) along the foot velocity $\boldsymbol{v}$. Note, when deriving the null space vector above, we assumed the angular velocity of the foot to be zero. Hence, the last three components of twist $\boldsymbol{t}$ all are zero, and the related terms have not been included in the above null space vector components. The reason is that necessary changes in foot orientation will be done separately, as explained later.

C. Singularity-consistent method applied to the support leg

The base frame is attached to the foot and is centered at the ankle joint. Joints are numbered sequentially, q_1 being closest to the foot.

When deriving the Jacobian, we make use of the fact that the hip joint assembly is kinematically equivalent to a spherical joint. That is, a solution similar to the well known spherical wrist partitioned solution can be obtained. In short, the Jacobian matrix takes the form as shown below:

$$\boldsymbol{J}(\boldsymbol{q}) = \begin{bmatrix} \boldsymbol{B} & \boldsymbol{0} \\ \boldsymbol{C} & \boldsymbol{D} \end{bmatrix}. \tag{12}$$

The zero submatrix in the upper right shows that joint speeds $\dot{q}_4$, $\dot{q}_5$ and $\dot{q}_6$ do not contribute to the velocity of the hip joint center point. Further on, from the velocity relation (1), we obtain:

$$\boldsymbol{v} = \boldsymbol{B}\dot{\boldsymbol{q}}_{123} \tag{13}$$

where $\dot{\boldsymbol{q}}_{123} = [\dot{q}_1\ \dot{q}_2\ \dot{q}_3]^T$, and $\boldsymbol{v}$ denotes the velocity of the hip joint center. Hence,

$$\dot{\boldsymbol{q}}_{123} = \boldsymbol{B}^{-1}\boldsymbol{v}. \tag{14}$$

We note that whenever the knee is extended ($q_3 = 0$), matrix $\boldsymbol{B}$ will be singular. The problem is adressed by reformulating the inverse kinematics, as in the last equation, in accordance with the Singularity-Consistent method. Following the steps as in Section II, we obtain the three elements of the null space vector $\boldsymbol{n}^{123}$:

$$\begin{aligned} n_1^{123} &= \frac{1}{C_2}\,(t_y C_6 + t_x S_6)\, S_4 S_{345} \\ n_2^{123} &= C_{345}\,(t_x S_6 + t_y C_6)\, S_4 \\ n_3^{123} &= -2C_{\alpha 5} C_\alpha\,(-(t_x C_5 C_6) + t_y C_5 S_6 + t_z S_5) \\ &\quad + (t_x S_6 + t_y C_6)\, S_4 S_{345} \frac{S_2}{C_2}. \end{aligned} \tag{15}$$

The Singularity-Consistent version of Eq. (14) becomes then:

$$\dot{\boldsymbol{q}}_{123} = b\boldsymbol{n}^{123}, \tag{16}$$

where b is an arbitrary scalar to be determined later.

Thereafter, the angular velocity of the upper body is found via:

$$\boldsymbol{\omega} = \boldsymbol{C}\dot{\boldsymbol{q}}_{123} + \boldsymbol{D}\dot{\boldsymbol{q}}_{456}$$

as

$$\dot{\boldsymbol{q}}_{456} = \boldsymbol{D}^{-1}(\boldsymbol{\omega} - \boldsymbol{C}\dot{\boldsymbol{q}}_{123}). \tag{17}$$

In contrast to solution (14), it can be shown that the kinematic singularity that would lead to rank deficiency of matrix $\boldsymbol{D}$ is out of the workspace of the leg. Hence, the above solution for $\dot{\boldsymbol{q}}_{456}$ can be directly applied. Since we assume constant orientation for the upper body for the time being, we have $\boldsymbol{\omega} = \boldsymbol{0}$. Inserting joint velocity (16) into the last equation, we obtain the three elements of the null space vector $\boldsymbol{n}^{456}$ for the hip joints q_4, q_5 and q_6:

$$\begin{aligned} n_1^{456} &= 2C_\alpha^2\left(2C_{\alpha 5}^2\,(-t_x C_6 + t_y S_6) + t_z \sin(2q_5 + q_4)\right) \\ n_2^{456} &= -2C_{\alpha 5} C_\alpha\,(C_{45}\,(-t_x C_6 + t_y S_6) + t_z S_{45}) \\ n_3^{456} &= -S_4\,(t_x S_6 + t_y C_6) \end{aligned} \tag{18}$$

and finally,

$$\dot{\boldsymbol{q}}_{456} = b\boldsymbol{n}^{456}. \tag{19}$$

where $\dot{\boldsymbol{q}}_{456} = [\dot{q}_4\ \dot{q}_5\ \dot{q}_6]^T$.

D. Hybrid control approach

When adapting the Singularity-Consistent method, there is a problem that for a specific end-effector twist $\boldsymbol{t}$, the null space vector vanishes totally. More specifically, this situation occurs at the extended leg singularity, when $\boldsymbol{t}$ is tangent to the leg motion outer boundary. This case is depicted in Fig. 3. This means that with the method, it is impossible to obtain foot motion that would trace out the boundary, and hence, stay at the singularity for a while. That is, a motion such that the leg would rotate in the hip while maintaining its fully stretched configuration. Note that such motion is typical for human walk [4]–[6]. Fortunately, there is a straightforward

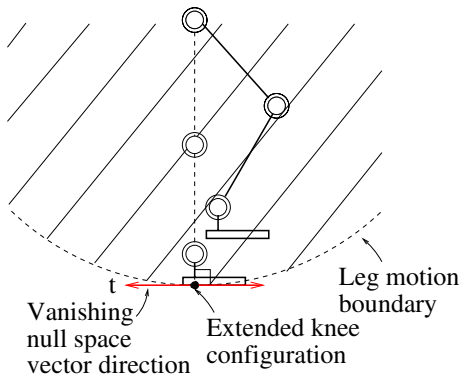

Fig. 3. Condition for vanishing null space vector.

solution to this problem. Whenever stretched-leg motion is

needed, ankle joint control can be directly applied. In this way, we obtain a hybrid control framework, such that approach and departure from the singularity is done via the Singularity-Consistent method, while motion along the singularity (outer boundary) is controlled directly in joint space (see Fig. 4).

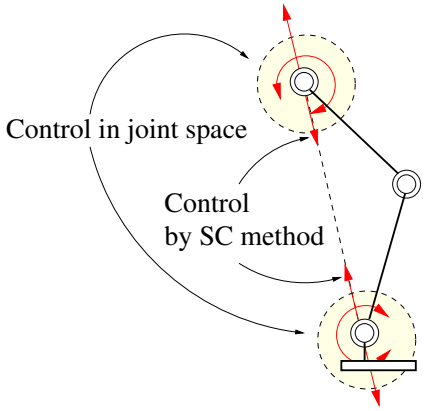

Fig. 4. Hybrid control approach.

IV. Experiments

Here we describe the implementation of our hybrid control approach for achieving *static walk*. We focus thereby on two main points: (1) realization of the hybrid control approach by means of *motion primitives*, and (2) the importance of *static stability margin*.

A. Motion Primitives

Statically stable cyclic walk will be generated by repeating a fixed cycle of motion primitives. These motion primitives are defined as follows (see also Fig. 5):

1) Initial position.
2) Move CoM over the left foot.
3) Lift the right foot.
4) Combined motion primitive:
   - shift CoM to center;
   - lower the right foot;
   - push body forward by left leg.
5) Move CoM over right foot.
6) Lift the left foot and align with right leg.
7) Combined motion primitive:
   - shift CoM to center;
   - lower the left foot;
   - push body forward by right leg.
8) Move CoM over the left foot.
9) Lift the right foot and align with left leg.
10) Lower the right foot.
11) Shift CoM to center (back to initial position).

In this context, Singularity-Consistent control is used to lift and to lower the feet. All other motion primitives are done by joint space control, using properly selected reference joint angles and 5th-order splines.

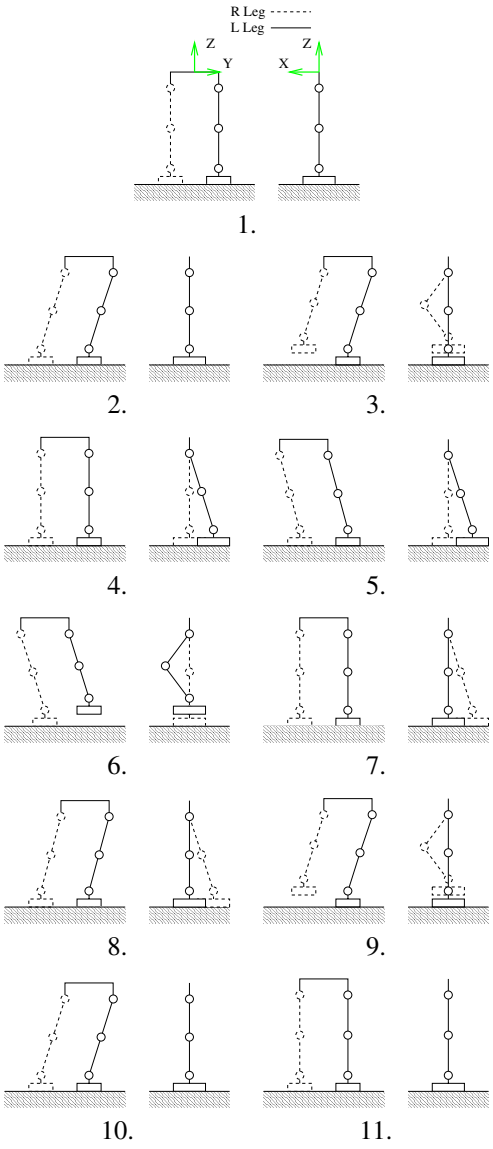

Fig. 5. Motion primitives.

B. Static stability

To realize the hybrid control approach by motion primitives, we need to select reference joint angles for the joint space control part. This we have done by determining beforehand the static stability margin of HOAP-2 experimentally. Static stability margins have been obtained while the robot balances on its left/right foot, for (1) leaning forward/backward and (2) leaning to the left/to the right. Thereby, the respective joint was rotated with a speed of 1 pulse/ms (4.78 deg/s) until balance is lost. Loss of balance is judged upon sensor data from the four pressure sensors mounted on each foot. Through these sensors, the reaction force and the location of the center of pressure (CoP) have been obtained. Loosing balance means that the reaction force will change abruptly.

Figures 6 and 7 show the reaction and the CoP position for each case. It is seen that with the change of the respective joint angle, the CoP first moves outward and then stabilizes for a while at the edge of the foot. Then, the reaction force

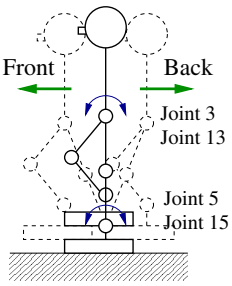

One leg balance and leaning forward/backward.

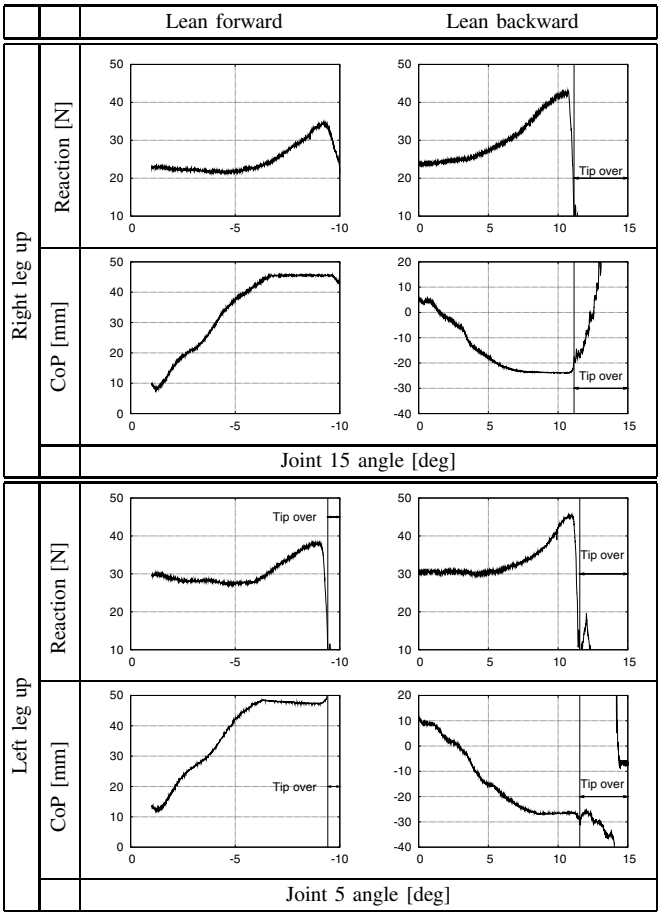

Fig. 6. Data on static stability when leaning forward and backward

changes abruptly and the robot tips over.

Static stability margins are then determined to be those joint angle values at which the CoP just begins to stabilize, at the foot edge (see Table I).

TABLE I

STATIC STABLITY MARGINS FOR HOAP-2

Initial position	Direction of motion	Stability interval
RLeg up	Front	$\geq$ -6.68 [deg]
	Back	$\leq$ 7.86 [deg]
	Left	stable in whole motion
	Right	$\geq$ 9.97 [deg]
LLeg up	Front	$\geq$ -6.18 [deg]
	Back	$\leq$ 8.38 [deg]
	Left	$\leq$ -10.54 [deg]
	Right	stable in whole motion

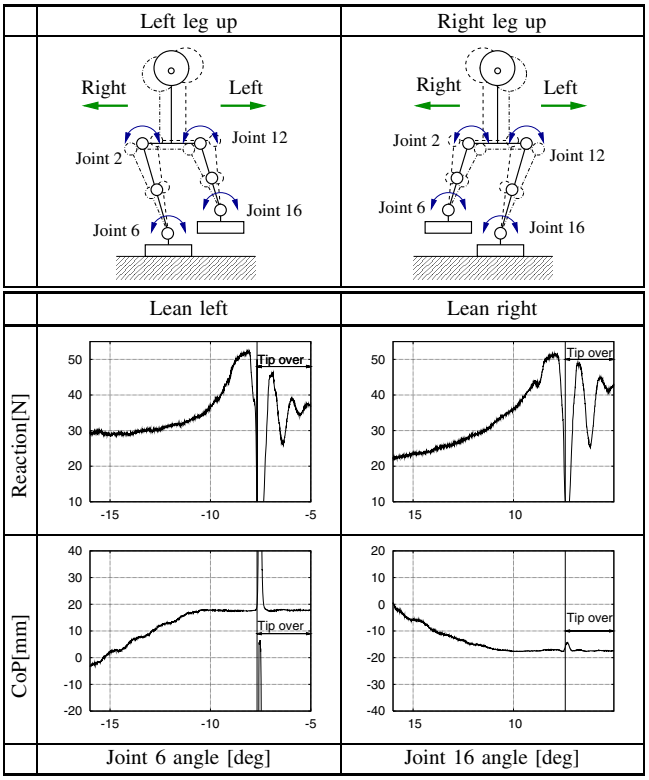

Fig. 7. Data on static stability when leaning right and left

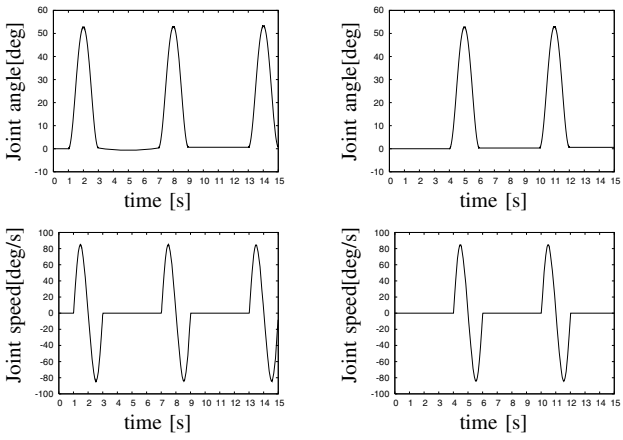

Fig. 8. Knee motion data for (a) left leg, (b) right leg

C. Command data and resulting motion

The commanded data are summarized in Table II. It is seen that the parameter b, appearing in the Singularity-Consistent (SC) method, has been selected as the sine function: $b = 4\sin\omega t$, where t is the elapsed time and $\omega = 2\pi/T$ and $T = 1$ s. The direction vector $\boldsymbol{t}$ has only a vertical component to lift/lower the foot, denoted as t_z. The angle data are reference angles for the respective joints. Based on these data, smooth joint trajectories were generated via 5th order splines.

Sensor data from the knee joints are shown in Fig. 8. From the joint angle data it is clearly seen that the legs have been fully stretched (knee joint angles zero), without any instabilities. Smooth walk has been achieved, which is apparent also from the snapshots in Fig. 9.

TABLE II

COMMAND DATA.

	Joint space			SC method	
MP	Leg	Joint number	values [deg]	t_z	b
2	Right	2	-2.5 → -16.0		
		6	2.5 → 16.0		
	Left	12	2.5 → -12.0		
		16	-2.5 → 12.0		
3	Right	3	0 → -5.0	-1	$4\sin\omega t$
		5	-1.0 → 5.0		
	Left				
4	Right			1	$4\sin\omega t$
	Left	13	0.0 → 5.0		
		15	-1.0 → -5.0		
5	Right	2	-16.0 → 12.0		
		6	16.0 → -12.0		
	Left	12	-12.0 → 16.0		
		16	12.0 → -16.0		
6	Right	3	-5.0 → 0.0		
		5	5.0 → 0.0		
	Left	13	5.0 → -5.0	-1	$4\sin\omega t$
		15	-5.0 → 5.0		
7	Right	3	0.0 → 5.0		
		5	0.0 → -5.0		
	Left			1	$4\sin\omega t$
8	Right	2	12.0 → -16.0		
		6	-12.0 → 16.0		
	Left	12	16.0 → -12.0		
		16	-16.0 → 12.0		
9	Right	3	5.0 → -5.0	-1	$4\sin\omega t$
		5	-5.0 → 5.0		
	Left	13	-5.0 → 0.0		
		15	5.0 → 0.0		
10	Right	3	-5.0 → 0.0	1	$4\sin\omega t$
		5	5.0 → -1.0		
	Left	13	0.0 → 0.0		
		15	0.0 → -1.0		
11	Right	2	-16.0 → -2.5		
		6	16.0 → 2.5		
	Left	12	-12.0 → 2.5		
		16	12.0 → -2.5		

V. CONCLUSIONS

We proposed a method to generate static walk of a humanoid robot with fully extended knees. The method is a hybrid in the sence that both inverse kinematics based on the Singularity-Consistent method, and joint space control is used. In the near future we intend to extend the results to a dynamic walking pattern. We believe also that such walk will increase energy efficiency and will be a naturally looking one.

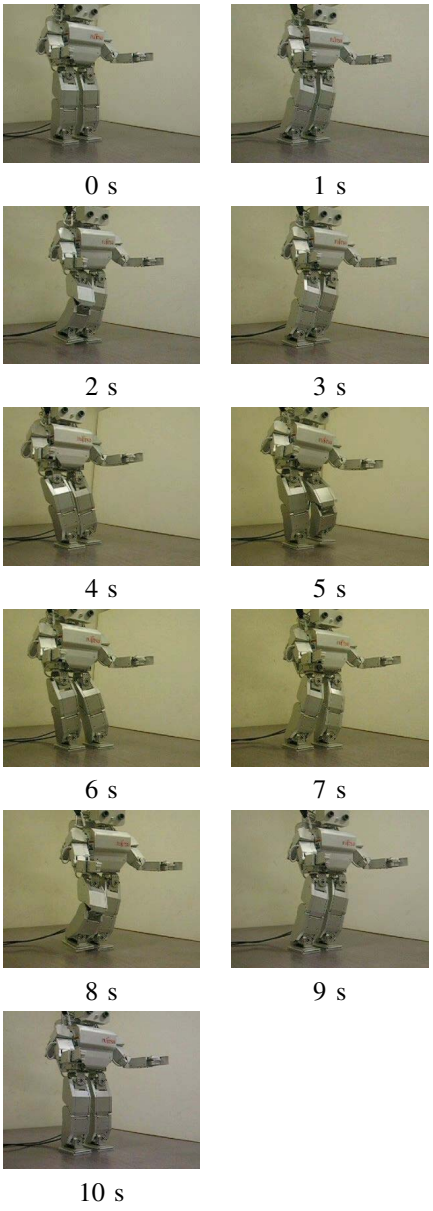

Fig. 9. Motion snapshots of walk with static stability.

REFERENCES

[1] M. Vukobratovich, B. Borovac, D. Surla and D. Stokic, "Biped Locomotion, Stability, Control and Application," Springer Verlag, 1990.

[2] S. Kajita, F. Kanehiro, K. Kaneko and K. Fujiwara, "Biped Walking Pattern Generation by using Preview Control of Zero-Moment Point," in Proc. 2003 IEEE Int. Conf. on Robotics and Automation, Taipei, Taiwan, September 2003, pp. 14–19.

[3] T. Sugihara, Y. Nakamura and H. Inoue: "Realtime Humanoid Motion Generation through ZMP Manipulation based on Inverted Pendulum Control," in Proc. 2002 IEEE Int. Conf. on Robotics and Automation, Washington, DC, May 2002, pp. 1404–1409.

[4] A. Sekiguchi, Y. Atobe, K. Kameta, Y. Tsumaki, D. N. Nenchev, "On Motion Generation for Humanoid Robot by the SC Approach," The 21th Annual Conference of the Robotics Society of Japan, 2A27, 2003.

[5] D. N. Nenchev, Y. Tsumaki and A. Sekiguchi, "Motion Feedback Control at a Singular Configuration," 4th SICE System Integration Chapter Conf., Dec. 19–21, 2003, Tokyo, Japan, pp. 508–509.

[6] Y. Ogura, T. Kataoka, K. Shimomura, H. Lim, A. Takanishi, "A Novel Method of Biped Walking Pattern Generation with Predetermined Knee Joint Motion," in Proc. 2004 IEEE/RSJ Int. Conf. on Inteligent Robotics and Systems, 2004, pp. 2381–2386.

[7] M. Morisawa, S. Kajita, K. Kaneko, K. Harada, F. Kanehiro, K. Fujiwara, H. Hirukawa "Pattern Generation of Biped Walking Constrained on Parametric Surface ," in Proc. 2005 IEEE Int. Conf. on Robotics and Automation, Barcelona, Spain, April 2005, pp. 2405–2410.

[8] R. Kurazume, S. Tanaka, M. Yamashita, T. Hasegawa, "Straight Legged Walking of a Biped Robot," in Proc. 2005 IEEE/RSJ Int. Conf. on Inteligent Robotics and Systems, 2005, pp. 3095–3101.

[9] D. N. Nenchev, Y. Tsumaki and M. Uchiyama, "Singularity-Consistent Parameterization of Robot Motion and Control," The International Journal of Robotics Research, Vol. 19, No. 2 pp. 159–182, 2000.

[10] K. Kameta, A. Sekiguchi, Y. Tsumaki, D. N. Nenchev, "Walking Control Using the SC Approach for Humanoid Robot," in Proc. IEEE-RAS Int. Conf. on Humanoid Robots (Humanoids 2005), pp. 289–294.

[11] Y. Tsumaki, D. N. Nenchev and M. Uchiyama, "Jacobian Adjoint Matrix Based Approach to Teleoperation," Int. Symp. on Microsystems, Intelligent Materials and Robots, Sendai, Japan, pp. 532–535, 1995.

[12] Fujitsu Automation Co., Ltd, Miniature Humanoid Robot HOAP-2 Instruction Manual.